Ion Flux Measurements in Electron Beam-Generated Plasmas

S.G. Walton, SFA, Inc., Largo, MD; D. Leonhardt, R.F. Fernsler, and R.A. Meger,
Naval Research Laboratory, Washington, DC

Key Words: Plasma species, Ion sources, Electron beam sources, Hollow cathode

ABSTRACT

Pulsed, electron-beam generated plasmas have been produced in Ar, N_2, and mixtures of Ar with N_2 and SF_6. The results of mass- and energy-resolved ion flux measurements at electrode surfaces located adjacent to these plasmas are presented as a function of operating pressure and gas composition. The results illustrate some of the unique features of electron beam generated plasmas.

INTRODUCTION

In processes ranging from etching to deposition, control over the flux of ions, neutrals, and reactive species to the surface as well as the energy at which they impact the surface is critical. The flux at the surface depends on the bulk plasma properties such as gas composition, plasma density, electron temperature, and the substrate location relative to the plasma source. Thus, control over the flux at substrate surfaces requires an ability to control the bulk plasma properties.

The Naval Research Laboratory is developing a new type of plasma source based on electron beam ionization. A magnetically confined, high-energy electron beam is used to ionize a background gas, thus producing a high-density ($> 10^{11}$ cm^{-3}) plasma over the volume of the beam [1].

There are several features that separate electron beam generated plasmas from conventional sources, most of which are derived from the fact that the electron beam drives the ionization process [2].

Low electron temperature. Typical electron temperatures are found to be less than 1.5 eV [1]. Electrons created in the ionization process are cooled by elastic and inelastic collision and not heated by external fields since they are not required to sustain the discharge.

Localized plasma source. The plasma production region is limited to the beam volume, which is well defined and characterized by high plasma densities. Outside the beam channel the temperature, density, and ion composition are altered by ion-neutral and ion-electron reactions. Since the electron beam is not tied to the chamber geometry, electrodes (or substrates) can be independently positioned to take advantage of the changes in the outwardly diffusing plasma.

Ion production. Electron beam ionization has the potential to generate a large distribution of ion species. The creation of ion species is determined by the partial cross sections for electron-impact ionization, and in a gas mixture, the relative ion densities will be approximately proportional to the mixture ratios.

These attributes allow for a high level of control over the flux of particles at the substrate. In this paper, experiments designed to quantify these features will be discussed [3]. The results of mass-resolved ion energy distributions measured at electrode surfaces located adjacent to pulsed plasmas produced in Ar, and N_2 and their mixtures are presented. Mass- and energy-resolved flux measurements in Ar/SF_6 mixtures are presented as well. Measurements are time-resolved and taken at a grounded and biased electrode as a function of operating pressure and gas composition. The results are discussed in terms of the fundamental plasma parameters and the relevant gas phase kinetics.

EXPERIMENTAL APPARATUS

Plasma Chamber

The experimental apparatus is schematically represented in Figure 1. The plasma chamber is approximately 70 cm long, 25 cm tall, and 100 cm wide (into the page). The vacuum is maintained by a 2000 *l*/s turbomolecular pump and the chamber base pressure is ~ $1x10^{-8}$ Torr. Gases are introduced via mass flow controllers and all gases are at least 99.9% pure. Operating pressures are achieved by selecting a flow rate and varying the conductance through a manual gate valve at the entrance to the pump. External to the chamber are magnetic field coils that produce a 150 Gauss field along the center of the chamber. The field strength varies by less than 10% over the region of interest.

Plasma Production

The electron beam was extracted from a linear hollow-cathode. The cathode was driven by a negative voltage pulse and generates a sheet-like electron beam commensurate to the applied voltage. The emergent beam, collimated by the mag-

© 2002 Society of Vacuum Coaters 505/856-7188
45th Annual Technical Conference Proceedings (2002) ISSN 0737-5921

netic field, passed through a slot in a grounded anode located downstream from the hollow-cathode and then terminated at a grounded beam dump. The electron beam volume between the slotted anode and dump defines the plasma source, with the dimensions set by the slot size (1 cm x 25 cm) and the anode-to-beam dump length (43 cm). For all measurements reported here the beam pulse was 2 ms long with a repetition rate of 50 Hz, and the beam energy was nominally 2 keV.

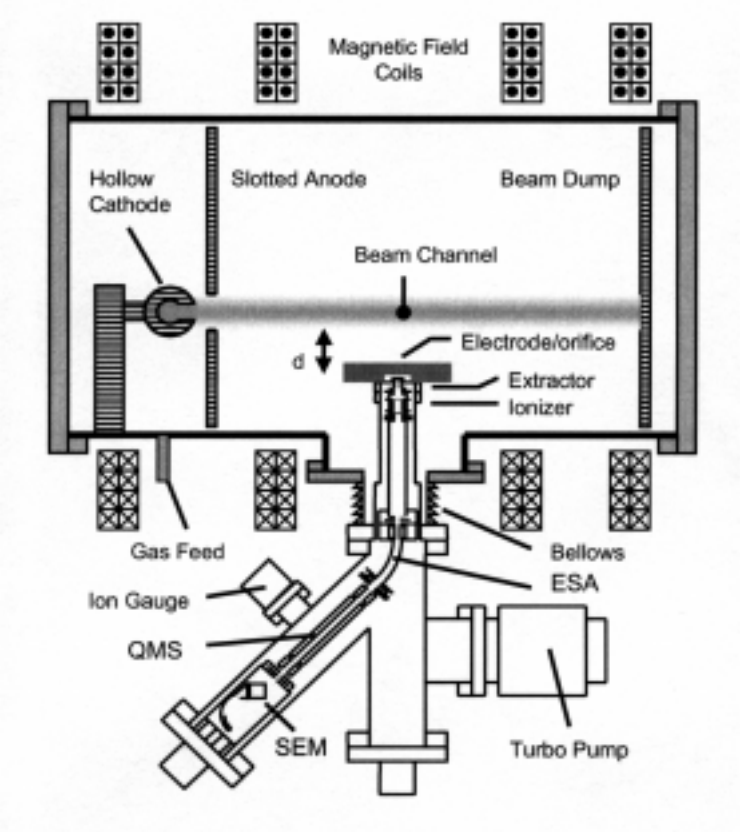

Figure 1: A Schematic diagram of the experimental apparatus.

Plasma Diagnostics

Ion fluxes and energy distributions were measured at the center of a 5.7 cm diameter stainless steel electrode using a Hiden EQP 300 Plasma Probe (Figure 1). The probe is differentially pumped and consists of an electrostatic ion-energy analyzer (ESA) in series with a quadrupole mass spectrometer (QMS). Ions enter the EQP through a 50 μm diameter aperture located in the center of the electrode and are then energy selected and mass filtered prior to detection by a channeltron secondary-electron multiplier (SEM). The resolution of the ESA is ± 0.15 eV. The EQP has not been calibrated to determine the absolute flux of each species and so the intensity of the measured signal is reported in arbitrary units. However, it is reasonable to compare relative signal intensities when the probe settings are held constant.

Time resolution was achieved using both a fixed and scanning gate on the EQP output (SEM). A fixed gating of the detector was used for accumulating the energy distributions. A 25 μs gate of the SEM signal was scanned in increments of 25 μs to obtain the temporal flux measurements. For both methods, the signal was accumulated over several hundred pulses to achieve a reasonable signal-to-noise ratio.

RESULTS AND DISCUSSION

Argon and Nitrogen plasmas

Ion energy distributions (IEDs) were measured with the electrode located 1.0 cm from the edge of the electron beam in argon (Figure 2) and nitrogen (Figure 3) plasmas over a range of pressures (30 - 90 mTorr). The distributions were accumulated during a period that extended from 0.5 to 2.0 ms. The accumulation period was chosen in order to sample the flux only after the plasma reached steady state, i.e., to eliminate variations observed during both the plasma onset and afterglow [3]. The species shown for argon (Ar^+ and Ar^{2+}) and nitrogen (N^+ and N_2^+) are the only appreciable species observed.

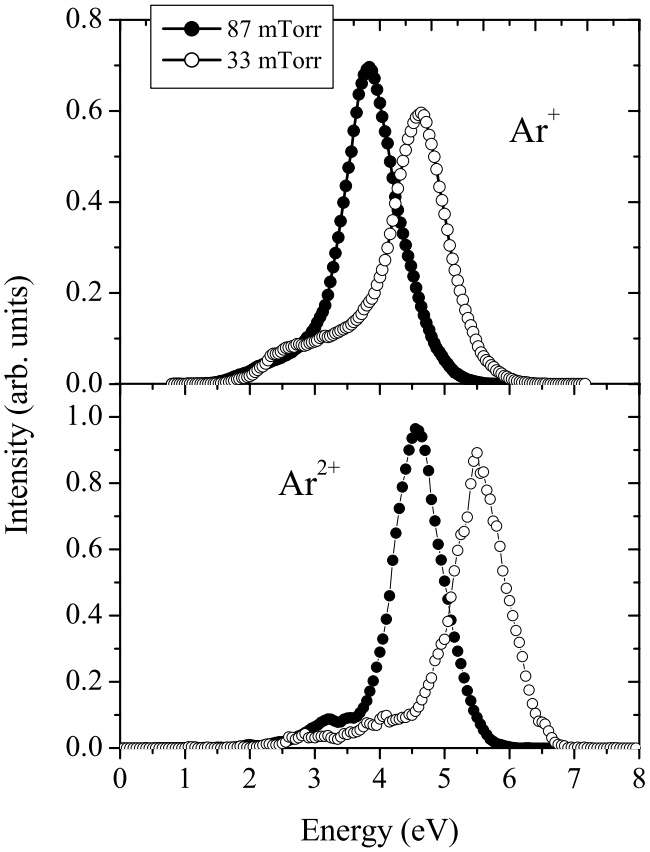

Figure 2: Kinetic energy distributions of Ar^+ (top) and Ar^{2+} (bottom) for plasmas produced in 33 and 87 mTorr of argon. The energy scale for Ar^{2+} has been halved for ease in comparison.

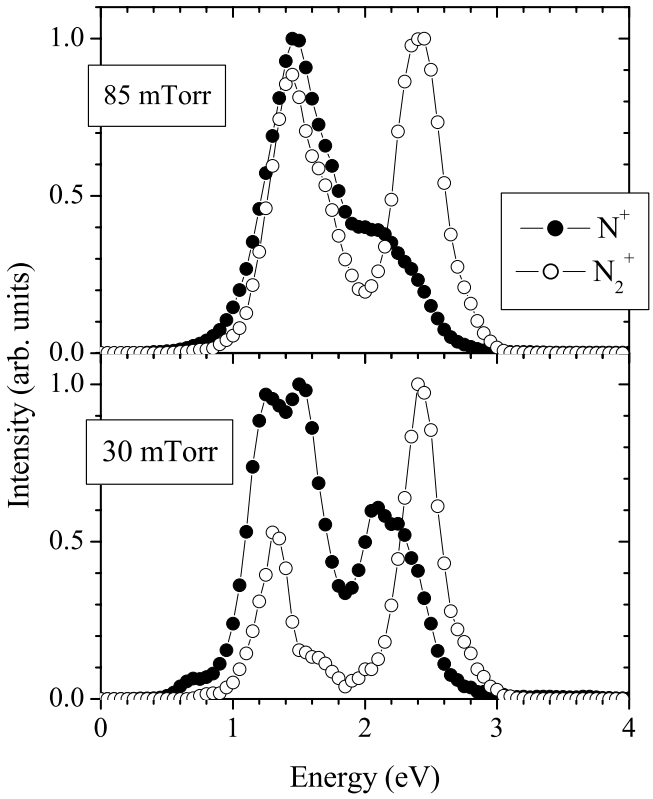

Figure 3: Kinetic energy distributions of N^+ and N_2^+ for plasmas produced in 85 mTorr (top) and 30 mTorr (bottom) of nitrogen.

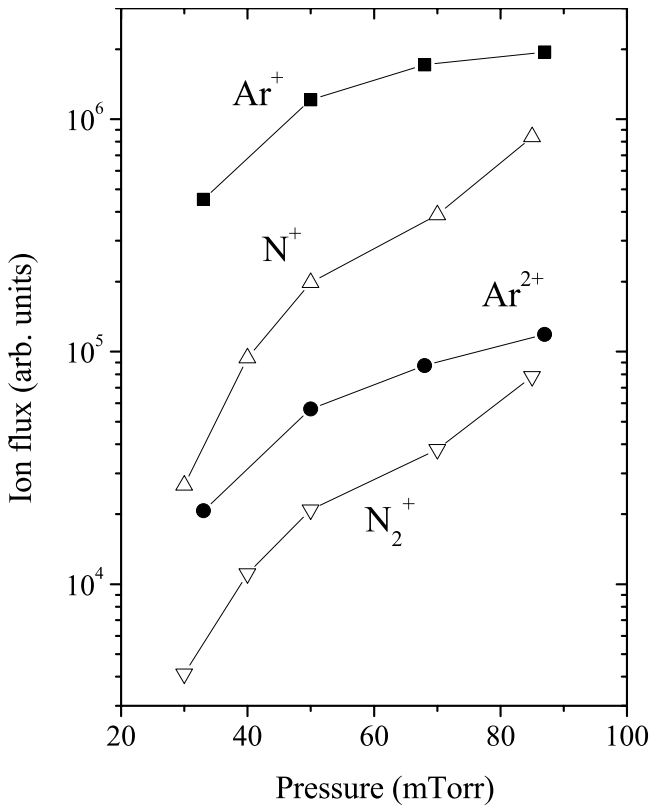

Figure 4: The ion fluxes in Ar and N_2 plasmas.

The flux of each ion species can be determined from the IED by integrating each IED. The fluxes are shown in Figure 4. The Ar^{2+} flux is ~ 5% of the Ar^+ flux and approximately equal to the ratio of partial cross sections for electron-impact ionization of Ar at 2 keV [4]. The N_2^+/N^+ flux ratio is ~ 10-15% and does not agree with the expected dissociative ionization fraction of $N^+/N_2^+ = 0.25$ for electron-impact ionization of N_2 [4]. This disparity will be addressed later.

IEDs not only yield information about the ion flux but can also be used to determine the plasma potential (ϕ) and the electron temperature (T_e), where ϕ is found to be proportional to T_e [5]. For an ion impacting a grounded electrode, the energy is equal to the potential at which the ion last collided. The highest energy ions are equal to $e\phi$, and from this energy we can calculate T_e. The results of these calculations are shown in Figure 5. The calculated electron temperatures are in good agreement with independent Langmuir probe measurements made in these sources [1].

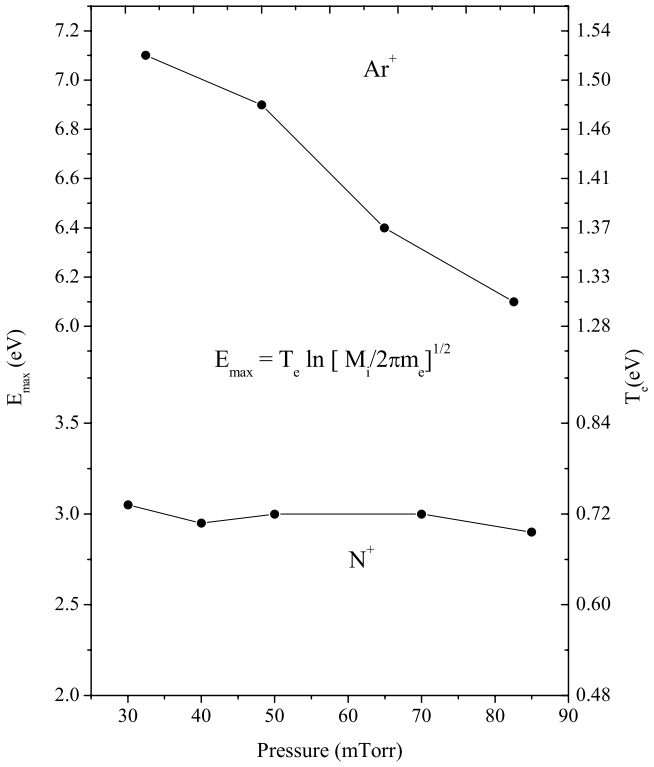

Figure 5: The maximum ion energies and calculated electron temperatures in Ar and N_2 plasmas.

The differences between the plasmas created in Ar and N_2 are apparent in their respective IEDs. Indeed, the IEDs in N_2 are bimodal and less energetic than the argon IEDs which exhibit single peak at higher energies. The characteristics of each plasma are understood in terms of the gas phase kinetics that govern the plasma dynamics. Plasma electrons are cooled via inelastic electron-neutral collisions. The threshold for molecular excitation in N_2 is ~ 0.3 eV while the lowest excited state in Ar is ~ 11 eV. This results in a lower T_e and φ and thus lower incident ion energies in N_2.

Consider now the effects of electron-ion recombination reactions such as $e + N_2^+ \rightarrow 2N$. In molecular gases, the electron-ion recombination rates are considerably higher than in atomic gases, where the process is three-body. This results in a rapid decrease in the N_2^+ density (and plasma density) outside the source region. This can explain the apparent disparity in the N_2^+/ N^+ flux ratio mentioned above and could also explain the bimodal energy distributions. The potential across the plasma varies with plasma density as $\phi(x) = \phi_o + T_e \ln [n(x) / n_o]$, where ϕ_o and n_o are the peak plasma potential and density. For $T_e = 0.7$ eV, a four-fold drop in n(x) would produce a potential drop of ~ 1 V, which is the approximate difference between peaks in the IEDs. Ions that are born in the plasma middle and suffer no collisions strike the electrode with an energy equal to $e\phi_o$. Ions that suffer collisions outside the beam, however, arrive at with an energy equal only to the sheath drop or less.

In Ar, the principal loss mechanism is diffusion, which produces only small density and potential gradients. Ions created outside the source region in Ar are the result of resonant charge exchange reactions and at these pressures, the mean free path is estimated to be ~ 1 mm [6]. These reactions would explain the existence of a small low energy component in the Ar^+ energy distributions.

Plasmas produced in mixtures of Ar and N_2 show that the addition of molecular gas strongly effects the plasma. Shown in Figure 6 are the results of measurements made for various N_2 concentrations. The parameters are the same as before and the total pressure was held constant at 85 mTorr. The rapid reduction in ion energies with increasing N_2 indicates a strong effect on electron temperatures. With small amounts of N_2, T_e rapidly falls below 1 eV and approaches values in pure N_2. It is important to note the direct correlation between the Ar^+ and N^+ fluxes and the gas composition. As expected, the electron beam produces species densities in proportion to the relative gas concentration.

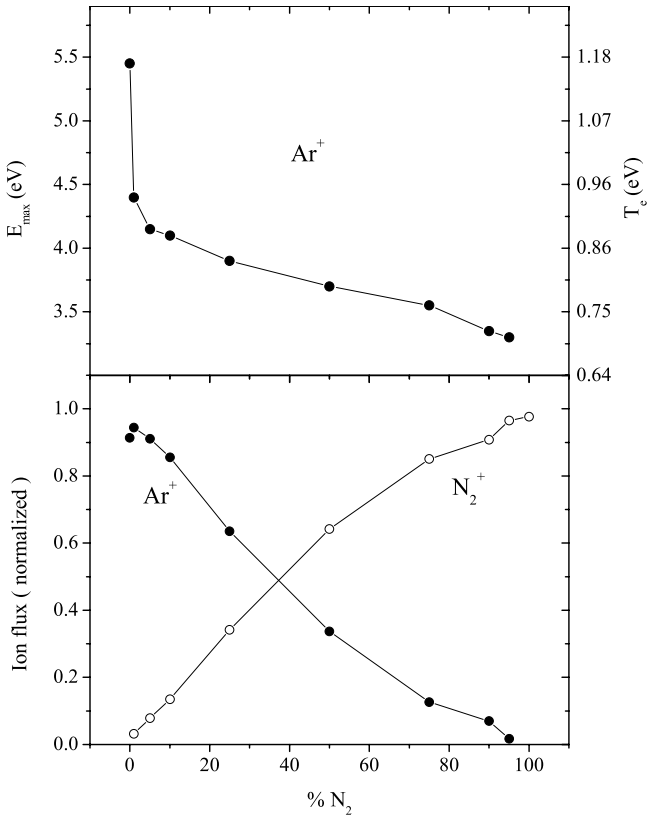

Figure 6: The maximum energies and relative fluxes in Ar/N_2 plasmas.

Ar/SF_6 mixtures

SF_6 is an electronegative gas with a large electron attachment ($e + SF_6 \rightarrow SF_6^-$) cross section, which increase as electron energies approach zero [7]. As shown above, T_e is less than 1 eV in N_2 and most Ar/N_2 mixtures. Because SF_6 is a molecular gas, Ar/SF_6 mixtures similarly have a low T_e and thus a large number of negative ions. If the negative ion production rate is large enough so that plasma electrons are rapidly converted to negative ions, the production of so-called ion-ion plasmas [8] are possible. In ion-ion plasmas the electron-to-negative ion ratio typically exceeds 1000. Ion-ion plasmas exhibit very different characteristics than conventional electron-ion plasmas and may have certain advantages in materials processing, based on the ability to deliver anisotropic fluxes of both positive and negative ions to the substrate.

Shown in Figure 7 are the spectra of positive and negative ions incident to the surface of an electrode located 1.0 cm from a plasma generated in a 70 mTorr, 50:50 mixture of Ar/SF_6. The

ions were extracted by applying a 2.0 kHz, square-wave bias of +/- 8 V to the electrode. Figure 8 shows the temporal variation in the extracted flux. Positive and negative ions are clearly extracted during the appropriate phase of the applied voltage. The temporal variations within each pulse and from pulse to pulse are not yet understood. Nonetheless, the ability to extract both negative and positive ions indicates that ion-ion plasmas are indeed formed.

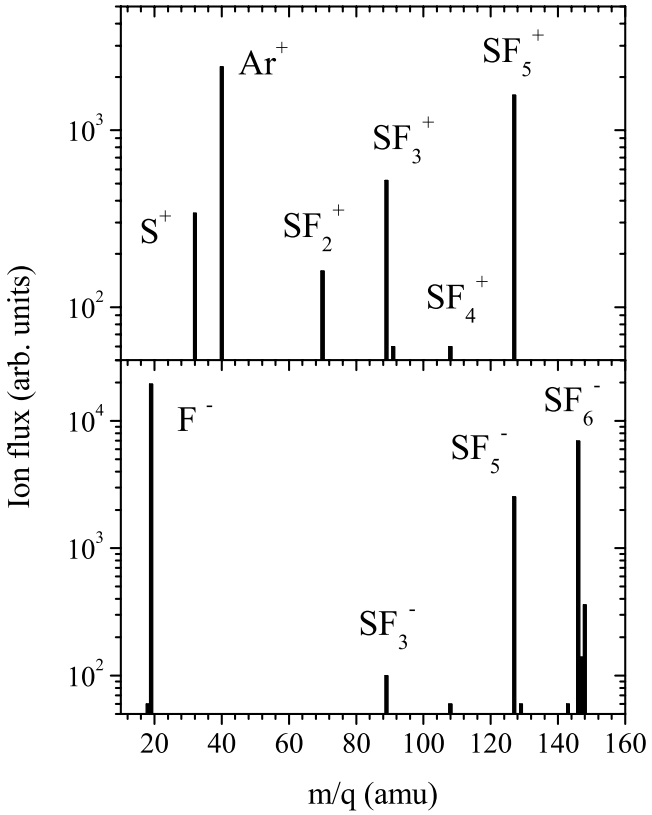

Figure 7: The spectra of positive (top) and negative (bottom) ions extracted from Ar/SF_6 plasmas.

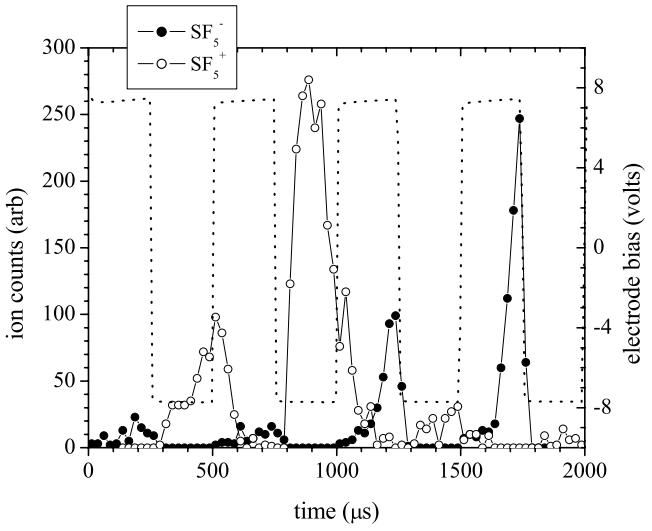

Figure 8: Temporal profile of SF_5^+ and SF_5^- extracted from Ar/SF_6 plasmas as well as the applied extraction bias.

SUMMARY AND CONCLUSION

Ion fluxes at electrodes located adjacent to pulsed, electron beam generated plasmas in noble and molecular gases have been measured. Ion energy distributions measured in Ar and N_2 over a range of pressures indicate very different plasma characteristics. The energies in N_2 are lower than the energies in Ar. Using the ion energies, the electron temperatures are estimated to be ~ 0.7 eV and ~ 1.3 - 1.5 eV in N_2 and Ar, respectively. In addition, the N_2 distributions are bimodal whereas the Ar distributions exhibit a single peak structure.

The measurements are partially understood in terms of electron beam ionization and the relevant gas-phase kinetics. The low incident ion energies result from a low electron temperature. This reduced electron temperature follows from the fact that the plasma electrons, in the absence of externally applied fields, are cooled through elastic and inelastic collisions. Since the threshold energy for excitation in N_2 is lower than the threshold in Ar, the electron temperatures are lower. This cooling mechanism is also observed in mixtures of Ar with N_2 and SF_6.

Electron-ion recombination plays a significant role in N_2 plasmas by destroying N_2^+ ions. This destruction is thought to produce strong plasma density and potential gradients and could lead to the measured bimodal energy distributions. It could also result in N^+ being the dominant ion measured at the surface. Since electron-ion recombination in Ar is negligible, ion loss is diffusion dominated and less dramatic, resulting in smoother decay and potential gradients. Hence, a single peak characterizes the ion energy distributions.

The low electron temperatures of these plasmas were coupled with a high electron attachment rate in Ar/SF_6 mixtures to study the formation of ion-ion plasmas. The formation of ion-ion plasmas were seen and validated by the simultaneous extraction of both positive and negative ions.

While the gas-phase reactions are specific to the gases described herein, it is reasonable to assume that plasmas will behave differently in atomic gases than in molecular gases. Furthermore, by choosing the appropriate gases and/or mixture ratios, gas-phase kinetics can add a certain level of control over the flux at substrates.

ACKNOWLEDGMENTS

This work was supported by the Office of Naval Research.

REFERENCES

1. D. Leonhardt, S.G. Walton, D.D. Blackwell, W.E. Amatucci, D.P. Murphy, R.F. Fernsler and R.A. Meger, "Plasma diagnostics in large area plasma processing system," *J. Vac. Sci. Technol.* A 19(4), 1367, 2001.

2. For an overview of electron beam-generated plasmas see: D. Leonhardt, M.M. Balkey, R.F. Fernsler, R.A. Meger, D.P. Murphy, S.G. Walton and D.D. Blackwell, "Plasma Processing System Based on Electron Beam Ionization," 45th Annual Technical Conference Proceedings of the Society of Vacuum Coaters, P-7, 2002; D. Leonhardt, "Electron-Beam Produced Plasmas: Considerations and Applications," *Vacuum Technology and Coatings*, 2 (11), 24-31 (2002).

3. Similar experimental work has been described in: S.G. Walton, D. Leonhardt, D.D. Blackwell, R.F. Fernsler, D.P. Murphy and R.A. Meger, *J. Vac. Sci. Technol*. A 19(4), 1325-1329 (2001); S.G. Walton, D. Leonhardt, D.D. Blackwell, R.F. Fernsler, D.P. Murphy and R.A. Meger, *Phys. Rev. E* 65, to be published (2002).

4. H.C. Straub, P. Renault, B.G. Lindsay, K.A. Smith and R.F. Stebbings, "Absolute partial cross sections for electron-impact ionization of argon from threshold to 1000 eV," *Phys. Rev. A* 52(2), 1115-1124 (1995); H.C. Straub, P. Renault, B.G. Lindsay, K.A. Smith and R.F. Stebbings, "Absolute partial cross sections for electron-impact ionization of H_2, N_2, and O_2 from threshold to 1000 eV," *Phys. Rev. A* 54(2), 2146-2153 (1995).

5. M.A. Lieberman and M.J. Lichtenberg, *Principles of Plasma Discharges and Materials Processing*, Chapter 6, John Wiley & Sons, New York, 1994.

6. A.V. Phelps, "Cross sections and swarm coefficients for nitrogen ions and neutrals in N_2 and argon ions and neutrals in Ar for energies from 0.1 eV to 10 keV," *J. Phys. Chem. Ref. Data* 20(3), 557-573 (1991).

7. L.E. Kline, D.K. Davies, C.L. Chen and P.J. Chantry, "Dielectric properties for SF_6 and SF_6 mixtures predicted from basic data," *J. Appl. Phys.* 50(11), 6789-6796 (1979).

8. For descriptions of ion-ion plasmas see: L.J. Overzet, B.A. Smith, J. Kebler and S.K. Kanakasabapathy, "Negative ion extraction from pulsed discharges," *Jpn. J. Appl. Phys.* 36(4b), 2443-2449 (1997); V. Midha and D.J. Economou, "Spatio-temporal evolution of a pulsed chlorine discharge," *Plasma Sources Sci. Technol.* 9, 256-269 (2000).